Available online at www.sciencedirect.com
SCIENCE DIRECT®
Geochimica et Cosmochimica Acta 70 (2006) 1636–1643
Geochimica
www.elsevier.com/locate/gca

Residence times for protons bound to three oxygen sites in the $AlO_4Al_{12}(OH)_{24}(H_2O)_{12}^{7+}$ polyoxocation

Jacqueline R. Houston [a], Brian L. Phillips [b], William H. Casey [a,c,*]

[a] Department of Chemistry, University of California, Davis, CA 95616, USA
[b] Department of Geosciences, State University of New York, Stony Brook, NY 11794, USA
[c] Department of Geology, University of California, Davis, CA 95616, USA

Received 23 August 2005; accepted in revised form 8 December 2005

Abstract

Although, the kinetic reactivity of a mineral surface is determined, in part, by the rates of exchange of surface-bound oxygens and protons with bulk solution, there are no elementary rate data for minerals. However, such kinetic measurements can be made on dissolved polynuclear clusters, and here we report lifetimes for protons bound to three oxygen sites on the $AlO_4Al_{12}(OH)_{24}(H_2O)_{12}^{7+}$ (**Al_{13}**) molecule, which is a model for aluminum-hydroxide solids in water. Proton lifetimes were measured using ^1H NMR at pH $\sim$ 5 in both aqueous and mixed solvents. The ^1H NMR peak for protons on bound waters (η-H_2O) lies near 8 ppm in a 2.5:1 mixture of H_2O/acetone-d_6 and broadens over the temperature range -20 to -5 °C. Extrapolated to 298 K, the lifetime of a proton on a η-H_2O is $\tau^{298} \sim 0.0002$ s, which is surprisingly close to the lifetime of an oxygen in the η-H_2O ($\sim$0.0009 s), but in the same general range as lifetimes for protons on fully protonated monomer ions of trivalent metals (e.g., $Al(H_2O)_6^{3+}$). The lifetime is reduced somewhat by acid addition, indicating that there is a contribution from the partly deprotonated **Al_{13}** molecule in addition to the fully protonated **Al_{13}** at self-buffered pH conditions. Proton lifetimes on the two distinct sets of hydroxyls bridging two Al(III) (μ_2-OH) differ substantially and are much shorter than the lifetime of an oxygen at these sites. The average lifetimes for hydroxyl protons were measured in a 2:1 mixture of H_2O/dmso-d_6 over the temperature range 3.7–95.2 °C. The lifetime of a hydrogen on one of the μ_2-OH was also measured in D_2O. The τ^{298} values are $\sim$0.013 and $\sim$0.2 s in the H_2O/dmso-d_6 solution and the τ^{298} value for the μ_2-OH detectable in D_2O is $\tau^{298} \sim 0.013$ s. The ^1H NMR peak for the more reactive μ_2-OH broadens slightly with acid addition, indicating a contribution from an exchange pathway that involves a proton or hydronium ion. These data indicate that surface protons on minerals will equilibrate with near-surface waters on the diffusional time scale.

1. Introduction

Geochemists are coming to rely heavily on computer methods of predicting reaction pathways in the Earth because so many of the key environments are difficult to sample. Particularly important are the reactions between minerals and aqueous solutions, as these reactions control the overall solution chemistry and the rates of mineral transformations. However, our ability to simulate such reactions is limited by a lack of experimental data at a suitable scale. Data are needed on *elementary* reactions, meaning reactions that proceed in solution as written on the molecular scale.

Work on aluminum-hydroxide molecules such as the $AlO_4Al_{12}(OH)_{24}(H_2O)_{12}^{7+}$ (**Al_{13}**) polyoxocation can be helpful in constraining the dynamic nature of functional groups at mineral surfaces. This molecule (Fig. 1) is among the best characterized aqueous oligomers, as the reactivities of structural oxygens (Phillips et al., 2000; Casey et al., 2000), the acid–base chemistry (Furrer et al., 1992), the dissolution rates (Amirbahman et al., 2000; Furrer et al., 1999) and pathways for oxygen-isotope exchanges (Rustad et al., 2004) are all known. From this work, we know that the 12 equivalent bound water molecules (η-H_2O) exchange with bulk solution in milliseconds when the

* Corresponding author. Fax: +1 530 752 1552.
E-mail address: whcasey@ucdavis.edu (W.H. Casey).

0016-7037/$ - see front matter © 2005 Elsevier Inc. All rights reserved.
doi:10.1016/j.gca.2005.12.007

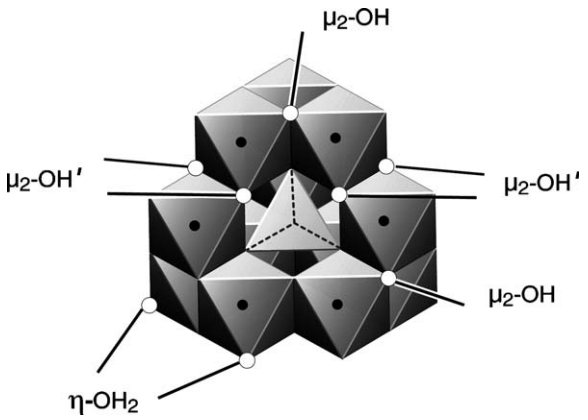

Fig. 1. Polyhedral representation of the $AlO_4Al_{12}(OH)_{24}(H_2O)_{12}{}^{7+}$ ion (**Al_{13}**), which has the ε-Keggin structure and three sets of structurally distinct protons on the fully protonated molecule.

molecule is fully protonated (pH < 6.5). The two structurally distinct sets of hydroxyl bridges within a single **Al_{13}** molecule (μ_2-OH, μ_2-OH′) exchange at rates that differ by a factor of $\sim 10^3$. At 298 K exchange of oxygen isotopes with bulk water occurs at characteristic times of $\tau^{298} \sim 1$ min and $\tau^{298} \sim 17$ h, assigned as μ_2-OH^{fast} and μ_2-OH^{slow}, respectively, although assignment to structural sites remains uncertain. Metal substitution into the core tetrahedral site causes enormous changes in reactivities of these hydroxyl bridges, but not the bound waters, which are virtually unchanged (Casey and Phillips, 2001; Lee et al., 2002a).

Timescales for dynamic conversion of functional groups determine how we should view their structures and even their stoichiometries. Consider, as an example, the $AlOH^{2+}$(aq) ion, which contains four bound water molecules in the inner-coordination sphere of the Al(III) and a single bound hydroxyl (see Swaddle et al., 2005). The bound hydroxyl interconverts back-and-forth to a water molecule by protonation/deprotonation $\sim 10^5$ times a second (Fong and Grunwald, 1969). Thus, on the timescale of a reaction that takes minutes to hours (e.g., polymerization and dissolution), it might be better to view the $AlOH^{2+}$(aq) ion as having five bound ligands, each one having the 4/5 the character of a bound water and 1/5 the character of a bound hydroxyl. The bound ligands are not static.

In this paper, we extend the earlier work of Akitt and Elders (1988) and Akitt (1989) and report rates of proton exchange from each of the different oxygen sites in the **Al_{13}** molecule (Fig. 1). Several authors have argued that molecules like the **Al_{13}** are useful for understanding some mineral surfaces, such as aluminum-hydroxide solids and clays (see Casey and Swaddle, 2003) because the **Al_{13}** is structurally similar to aluminum-hydroxide solids (Bradley et al., 1993; Phillips et al., 2000). It polymerizes to form a gel that ages to bayerite (see Bradley et al., 1993; Furrer et al., 2002) and the proton charge density of **Al_{13}** (0.32 C/m^2; +7 charge over a sphere with radius of 0.53 nm) is comparable to that of aluminum-hydroxide solids (0.16–0.48 C/m^2; Hiemstra et al., 1999). Thus, understanding proton residence times on the **Al_{13}** should be useful in understanding proton residence times at the surfaces of more complex and heterogeneous materials, such as aluminous clays, which should nonetheless expose structurally similar stoichiometries to the aqueous solution.

2. Materials and methods

2.1. Starting material

Synthesis of $Na[AlO_4Al_{12}(OH)_{24}(H_2O)_{12}(SeO_4)_4](H_2O)_x$ (**Al_{13}**) crystals was accomplished using the method of Furrer et al. (1992). For the variable-temperature experiments, 23 mg of **Al_{13}** selenate crystals were ground with excess $BaCl_2$ (~13 mg) and extracted with 500 μL of distilled water. This $BaCl_2$ solution metathetically dissolves the salt, precipitates the selenate, and releases the oligomer cation intact to solution. The resulting solution containing the **Al_{13}** cation was filtered through a 0.22 μm membrane filter into a 5-mm (o.d.) NMR tube. For measurements at low temperature, 200 μL of acetone-d_6 (dimethylketone: C_2D_6O) was added to the filtrate in order to depress the freezing point of the solution to as low as −20 °C. However, further additions of acetone-d_6 significantly decreases the solubility of **Al_{13}** in solution, which makes experiments at temperatures below −20 °C difficult. For the kinetic experiments performed above room temperature, a 2:1 mixture of water and dmso-d_6 (dimethylsulfoxide: C_2D_6SO) was used to raise the boiling point of a neat H_2O solution.

The pK_a of the **Al_{13}** molecule is near $6 < pK_a < 6.5$ (Furrer et al., 1992; Lee et al., 2002b) so extraction of this amount of the salt into water yields a solution near pH ~ 5 because a small fraction of waters bound to the **Al_{13}** deprotonate. To measure pH, glass electrodes were calibrated in the appropriate solvent on the concentration scale and pH values were measured at 298 K. For the experiments in which pH was varied, aliquots of HCl (0.1 M HCl) diluted with an appropriate amount of acetone-d_6 or dmso-d_6 were added to an amount of stock solution as the electrode response was measured.

2.2. ^1H NMR spectroscopy

All NMR measurements were conducted with a Bruker Avance NMR spectrometer based on an 11.7 T magnet located at the University of California Davis, NMR facility. ^{1}H NMR spectra were recorded at 500.1 MHz using a low-temperature 5-mm probe in locked mode (acetone-d_6 or dmso-d_6). A pulse width of 4 μs corresponding to a 33° tip angle ($\pi \approx 22$ μs based on the bulk water signal) was used with a relaxation delay of 1 s. Two hundred scans were recorded over a sweep-width of 7.5 kHz. Sample temperature was determined with a copper–constantan thermocouple placed inside a separate NMR tube but with similar geometry and with the same solvent mixture as

the samples. We estimate the error in the temperature readings to be much less than ±0.5 K.

Rates of proton exchange from the η-H_2O and μ_2-OH were determined using the dynamic NMR line-broadening technique by measuring the full-width of the peak at half-maximum. Line-shape parameters were calculated from least-squares fits of the frequency-domain data to Lorentzian curves using our own computer code, which compares well with commercial software. The proton mole fractions (p_j) were calculated from signal areas and are near the calculated populations based on the reagent concentrations.

2.3. Rate equations

There are three inequivalent proton sites in the **Al_{13}** (Fig. 1)—two sets of hydroxyl bridges and one set of bound waters, yielding a 1:1:2 stoichiometric ratio of hydrogen. Depending upon temperature, distinct signals can be observed for each bound proton site in the **Al_{13}** and proton transfer occurs in the slow-exchange regime because: $2 \cdot \pi \cdot \Delta\nu \gg k$, where $\Delta\nu$ is the frequency separation between the two signals in hertz (Hz) and k is the exchange rate constant (Sandström, 1982; Houston and Casey, 2005). Although there are at least four proton sites for exchange in the system (three sites on the **Al_{13}** and bulk water), we can assume that direct exchange between protons on the μ_2-OH and η-H_2O sites on the **Al_{13}** are unlikely and that exchange to the **Al_{13}** sites is solely via a bulk water molecule. With this assumption, we can treat the kinetics using two-site exchange with no loss of accuracy; that is, separate exchange occurs between each site on the **Al_{13}** and bulk water molecules. Although, Akitt and Elders (1988) observed an intramolecular proton exchange for **Al_{13}**, their measurements were conducted in purely non-aqueous solvent, with very low concentrations of solvent water.

The NMR lineshape for an exchanging two-site system can be calculated from the modified Bloch equations (see Bleuzen et al., 1997), given in matrix form:

$$V(\omega) = \sum \left[\begin{bmatrix} [(\omega - \Omega_A)\mathrm{i} - T_{2_A}^{-1} - k_A] & \frac{k_A p_A}{p_B} \\ k_A & \left[(\omega - \Omega_B)\mathrm{i} - T_{2_B}^{-1} - \frac{k_A p_A}{p_B}\right] \end{bmatrix}^{-1} \cdot \begin{bmatrix} p_a \\ p_b \end{bmatrix} \right], \quad (1)$$

where $V(\omega)$ is the calculated line shape for the exchanging site and the summation runs over the spectral frequency range. The terms $(\omega - \Omega_j)$, p_j, T_{2j}^{-1}, and k_j, correspond to the frequency offset (Ω_j is the chemical shift of the 'jth' site), the proton mole fraction of site j, the transverse relaxation rate of site j, and exchange-rate constant, k_j, respectively. Because we measure exchange in a state of dynamic equilibrium, the populations relate as: $p_A \cdot k_A = p_B \cdot k_B$. The exchange rate constants correspond to the inverse of the average lifetime of a proton in that site: $k_j = 1/\tau_j$.

Under the conditions $p_A \ll p_B$ and $k_A < |\Omega_A - \Omega_B|$, which applies to the system discussed here, Eq. (2) provides a good estimate of the rate coefficient (see Sandström, 1982; Houston and Casey (2005)):

$$k_j = \pi(\mathrm{FWHM}_j - \mathrm{FWHM}_o). \quad (2)$$

The term FWHM_j corresponds to the exchange-broadened line width and FWHM_o corresponds to the natural line width of that proton in the absence of exchange. The FWHM_j was determined by fitting the sum of Lorentzian curves after subtracting the peak that corresponds to the dominant bulk-water resonance. We estimated FWHM_o from the width of the resonance from methyl protons in the organic solvent to be ~2–3 Hz, which are unreactive at these conditions. (We also use this estimate of FWHM_o in experiments with neat D_2O.) Because this line width is reasonably small compared to the line width of the exchange-broadened peak (i.e., FWHM(η-H_2O) > 100 Hz), calculation of the rate constant was done using the FWHM_j only. This assumption is fully justified for most of the sites because the line widths are much larger than the ~2–3 Hz that we estimate as the instrumental line width. The assumption may be poor for the slowly exchanging hydroxyl bridge, where the linewidth is 7–10 Hz, but still yields rate constants within the millisecond range.

Activation parameters were derived from the variation in rate constant (k_j) with temperature, in accordance with the Eyring equation:

$$\frac{1}{\tau} = k_{j,\mathrm{ex}} = \frac{k_b \cdot T}{h} \mathrm{e}^{\frac{\Delta S_j^{\ddagger}}{R}} \mathrm{e}^{\frac{-\Delta H_j^{\ddagger}}{RT}}, \quad (3)$$

where k_b is the Boltzmann constant and the exponential terms include the activation entropy $[\Delta S_j^{\ddagger}]$ and activation enthalpy $[\Delta H_j^{\ddagger}]$ for chemical exchange at the jth species. The parameters T, R, and h are absolute temperature, the gas constant, and the Planck constant, respectively.

3. Results

3.1. The *Al_{13}* solution

At temperatures lower than 273 K, the ^{1}H NMR spectrum of **Al_{13}** in a 2.5:1 mixture of H_2O/acetone-d_6 contains three peaks near +8, +4.5, and +3.8 ppm assigned to protons on the **Al_{13}** complex (Fig. 2), in addition to the dominant peak from solvent hydrogen (+5.4 ppm and small

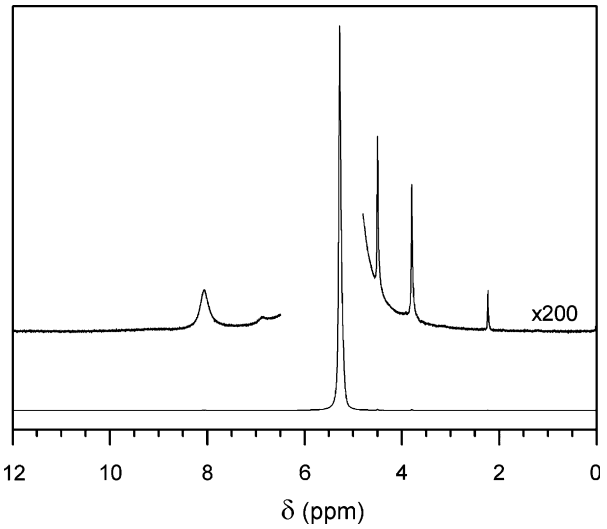

Fig. 2. ^{1}H NMR spectrum at −20.6 °C of $\mathbf{Al_{13}}$ dissolved in a 2.5:1 mixture of H_2O/acetone-d_6. Peaks corresponding to the dissolved $\mathbf{Al_{13}}$ are apparent at expanded vertical scale (upper trace). The spectrum is dominated by protons in bulk water near +5.4 ppm, as seen in the lower trace. The ordinate is intensity in arbitrary units and the two traces are offset vertically from one another for clarity.

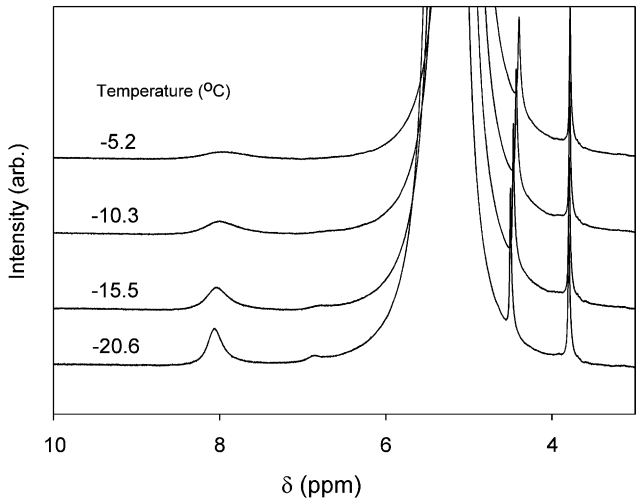

Fig. 3. ^{1}H NMR spectra of $\mathbf{Al_{13}}$ dissolved in a 2.5:1 mixture of H_2O/acetone-d_6 to depress the freezing point of the solution so that the η-H_2O could be observed (∼8 ppm). Peaks at 3.8 and 4.5 ppm correspond to the hydroxyl bridges. Spectra are plotted with a ∼200 expanded vertical scale.

peaks near 2 ppm from ^{1}H impurities in the deuterated acetone). A small peak was also detected near +6.8 ppm that cannot be assigned unambiguously, but could arise from $\mathbf{Al_{13}}$ decomposition products.

At conditions where all of the peaks are well resolved, the relative intensities (integrated areas) of the ^{1}H peaks assigned to the $\mathbf{Al_{13}}$ at +8, +4.5, and +3.8 ppm have approximate ratios 2:1:1, respectively. This observation suggests assignment of the peak near +8 ppm to protons in the bound water molecules and those of +4.5 and +3.8 ppm to bound hydroxyl groups (μ_2-OH or μ_2-OH′ in Fig. 1). These spectra and assignments are in close agreement with the results of Akitt and Elders (1988) for $\mathbf{Al_{13}}$ in nearly pure acetone-d_6 solvent. The area of the peak for the η-H_2O (with two protons each) should equal the sum of the area of the bound hydroxyls (two sets of 12 μ_2-OH, each with a single proton) by the molecular stoichiometry.

The ^{1}H NMR peak for η-H_2O in the 2.5:1 mixture of H_2O/acetone-d_6 (near 8 ppm) broadens substantially over the temperature range −20 to −5 °C (Fig. 3), in ways that can be directly interpreted via Eq. (2) to yield rate coefficients and proton lifetimes. At temperatures above −5 °C, the peak becomes undetectably broad because of rapid exchange of protons with solvent.

Peaks corresponding to the two sets of μ_2-OH in the 2.5:1 H_2O/acetone-d_6 mixture do not appreciably broaden with increased temperature over the temperature range −20 to −5 °C. The absence of broadening indicates that chemical-exchange rates are less than the natural line width of these sites, which equals a few hertz over this temperature range. We therefore employed a 2:1 solvent mixture of H_2O/dmso-d_6 to extend measurements to higher temperatures (3.7–95.2 °C) where acetone is too volatile, and augmented these measurements with spectra collected in nearly pure D_2O.

In the H_2O/dmso-d_6 mixture, the ^{1}H NMR peaks for both sets of hydroxyl bridges lie near 3.8 ppm, and overlap at temperatures below ∼10 °C (Fig. 4). With increasing temperature these peaks shift and separate until they are distinct from one another. The upfield peak broadens with increasing temperature, becoming nearly undetectable near 74 °C. At this temperature, the downfield peak remains

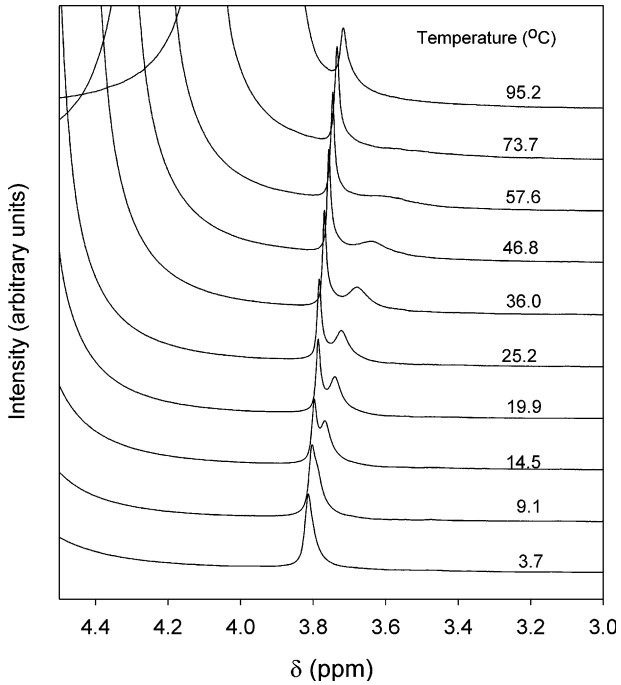

Fig. 4. ^{1}H NMR spectral region for μ_2-OH of $\mathbf{Al_{13}}$ dissolved in a 2:1 mixture of H_2O/dmso-d_6. Spectra were acquired over a wide temperature range, 3.7–95.2 °C, in order to observe exchange of the protons from both μ_2-OH. Spectra are plotted with a ∼200 times expanded vertical scale relative to the solvent-water resonance, which appears offscale and shifts from +4.8 to +4.05 ppm with increasing temperature.

distinct, although it has shifted upfield and broadened slightly. Shifting of the peak positions with temperature is caused by changes in the shielding properties of the solvent, not chemical exchange, and is expected in these solvents (e.g., Akitt and Elders, 1988). These line widths are plotted as a function of $1/T$ in Fig. 5 and the rate coefficients and activation parameters are compiled in Table 1.

One peak from the **Al_{13}** molecule is detectable in neat D_2O (Fig. 6), which we assign to a μ_2-OH site. The ^1H NMR signal, originating mostly as bulk water, arises from small amounts of proton contamination in the deuterated solvent and from protons carried into the solvent from extraction of the fully protonated $Na[AlO_4Al_{12}(OH)_{24}(H_2O)_{12}(SeO_4)_4](H_2O)_x$ crystals. The peak broadens with increasing temperature, as expected, and a least-squares fit of this temperature-dependence yields an estimate of

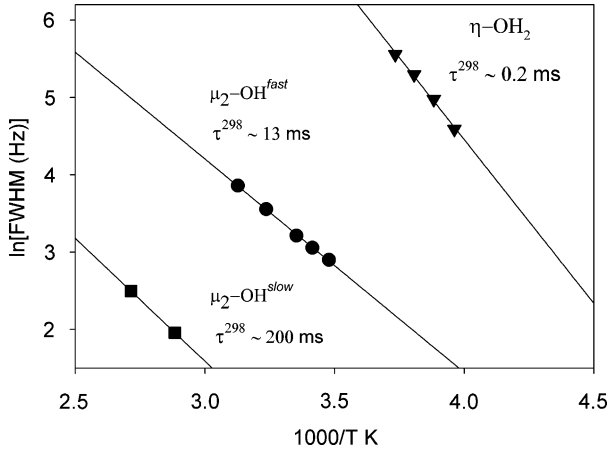

Fig. 5. Variation of line width with temperature for the η-H_2O (2.5:1 H_2O/acetone-d_6 solvent) and both μ_2-OH (2:1 H_2O/dmso-d_6 solvent) on **Al_{13}**. Also shown are the characteristic lifetimes for bound protons on the structural sites extrapolated to 298 K.

Table 1
Average lifetimes at 298 K (τ^{298}) and activation parameters for exchange of oxygens and protons between atom sites in the **Al_{13}** molecule and bulk solution

Site	τ^{298} (s)	$\Delta H^{\ddagger}$ (kJ mol^{-1})	$\Delta S^{\ddagger}$ (J mol^{-1} K^{-1})
Oxygen exchange by ^{17}O NMR, H_2O solvent			
η-OH_2	0.0009	53(±12)	−7(±25)
μ_2-OH^{fast}	62.5	202(±23)	403(±43)
μ_2-OH^{slow}	6.25×10^4	104(±20)	5(±4)
Proton exchange by ^1H NMR in mixed H_2O/organic solvent			
η-OH_2[a]	0.0002	33(±2)	−64.6(±7)
μ_2-OH^{fast} [b]	0.013	20.4(±1)	−140(±2)
μ_2-OH^{slow} [b]	0.201	23	−153
Proton exchange by ^1H NMR in D_2O solvent			
μ_2-OH^{slow} [c]	0.013	30.7(±1)	−106(±3)

The data for proton exchange come from ^1H NMR data, Eq. (3) and the relation: $1/\tau = k_{ex}$. Data for oxygen exchange by ^{17}O NMR are given in Phillips et al. (2000) and Casey et al. (2000).
[a] 2.5:1 H_2O/acetone-d_6 solvent.
[b] 2:1 H_2O/dmso-d_6 solvent.
[c] Tentative assignment.

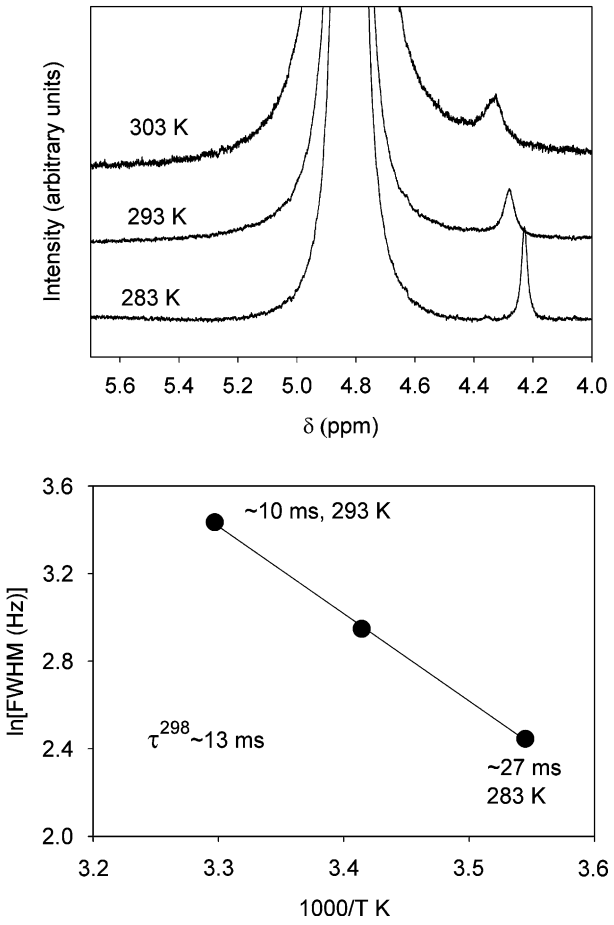

Fig. 6. ^1H NMR spectra (top) of the **Al_{13}** molecule dissolved in virtually pure D_2O with a signal corresponding to one of the μ_2-OH (~4.3 ppm). The line widths increase with temperature, as expected, and yield average lifetimes for the bound proton (bottom). The spectra are plotted at vertical exaggeration of ~1100 relative to the bulk-water peak.

$\tau^{298} = 0.013$ s (Fig. 6). If this peak corresponds to the μ_2-OH^{slow} site from the mixed solvents, then the rates increase by more than an order of magnitude when the mixed organic/aqueous solvent is replaced with a fully aqueous solvent. If the peak corresponds to the μ_2-OH^{fast} site, then the rates are virtually unchanged. We cannot unequivocally assign this peak to either the μ_2-OH^{fast} or μ_2-OH^{slow} site, but we suspect that it is from the μ_2-OH^{slow} site. Exchange rates are expected to depend on the concentrations of the exchangeable hydrogen in the solvent and no other resonance of comparable area intensity was observed that could be assigned to a more inert μ_2-OH site.

3.2. Upon acidification

The line width of two of the three ^1H NMR peaks from the **Al_{13}** molecule changes with acid addition, but in opposite directions (Fig. 7). The peak corresponding to the η-H_2O (~8 ppm) becomes increasingly narrow with decreasing pH and one of the peaks assigned to the μ_2-OH site broadens (Fig. 7). This broadening is evident in both water/dmso-d_6 and water/acetone-d_6 mixtures.

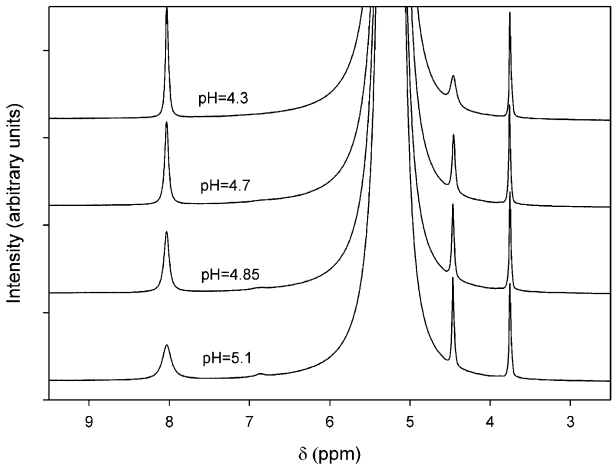

Fig. 7. ^{1}H NMR spectra of the **Al$_{13}$** molecule in 2.5:1 H_2O/acetone-d_6 solvent. The spectra were acquired at −16.9 °C and the solutions were acidified by adding small amounts of HCl at 298 K. The pH values were measured at 298 K on the concentration scale with an electrode calibrated in the mixed solvent. Vertical exaggeration is ~75 times relative to the bulk-water peak.

For the η-H_2O protons in the 2.5:1 water/acetone-d_6 solvent at −16.9 °C, an asymptotic approach to a constant line width (~22 Hz) is evident as pH is lowered (line widths decrease from ~66 to ~22 Hz over the pH range $4.3 < pH < 5.1$). Over approximately the same pH range, but at higher temperature (9.9 °C), line widths for η-H_2O protons in the 2:1 water/dmso-d_6 solution increase from ~145 to ~220 Hz. These data clearly indicate that the nature of the solvent affects the proton lifetimes, and that there is a contribution to proton exchange from the conjugate base of the **Al$_{13}$**. (Note that the temperatures in this comparison differ considerably.) This contribution decreases with acidification to $pH \ll pK_a$.

The peak assigned to the more reactive μ_2-OH also broadens slightly with acidification in 2:1 dmso-d_6 solution, from ~20 to ~86 Hz over the range $4.3 < pH < 5.0$ at 9.9 °C. It broadens from ~21 to ~37 Hz at $4.3 < pH < 4.9$ at −16.9 °C in the 2.5:1 water/acetone-d_6 mixture. Keeping in mind that the experiments were conducted in different solvents and at different temperatures, the broadening indicates a pathway for exchange that either involves a transient protonated μ_2-OH bridge, or proton transfer from an H_3O^+ ion. We cannot distinguish these two cases with the present data, although Furrer et al. (1999) argued from electrostatic calculations that the bridges could not be hyperprotonated. The line width for the less-reactive μ_2-OH is constant with pH over this range.

4. Discussion

There are several results that are important to our greater goal of understanding proton-transfer rates on geological materials. On the **Al$_{13}$**: (i) the proton lifetimes for a η-H_2O are in the millisecond to submillisecond range; (ii) the proton lifetimes on the two sets of μ_2-OH are much longer than for those on the bound waters and differ considerably from one another; (iii) proton lifetimes on a η-H_2O increase slightly upon acidification; (iv) proton lifetimes for one μ_2-OH site decrease slightly upon acidification; (iv) the lifetime for a proton on one μ_2-OH site is detectable in nearly pure D_2O and falls in the same general range as in the mixed aqueous/organic solvents.

4.1. Lifetimes of protons on bound waters (η-H_2O)

In general, one expects three pathways for proton exchange for a bound water molecule, leading to an expression for the net rate:

$$k = k_1 + k_2[H^+] + k_3/[H^+]. \quad (4)$$

The first pathway (k_1) corresponds to direct transfer of a proton from an inner- to an outer-sphere water and is constant with pH. The second term (k_2) describes the proton-enhanced pathway that becomes important at low pH when H_3O^+ ions are involved in proton transfer. However, for fully hydrated metals, this pathway is evident at much higher hydronium ion concentrations than we employ here. For example, no proton-enhanced pathway was observed for bound waters on the $Al(OH_2)_6^{3+}$ ion ($pK_a = 4.97$) even at $pH \sim 0.5$ (Fong and Grunwald, 1969). For the present results, we can probably ignore this pathway for the **Al$_{13}$** since line widths narrow as pH is lowered.

The third pathway, described by k_3, corresponds to proton transfer from the conjugate base of the **Al$_{13}$**, which becomes important at $pH \sim pK_a$ and above. Clearly, there is such a contribution for the **Al$_{13}$** molecule at the extracted pH, although the contribution is not large (Fig. 7). The lifetimes of protons on the η-H_2O are surprisingly long (0.2 ms) and further increase by a factor of 2–3 as the solution pH is decreased away from $pH \sim pK_a$. Rates are likely to be faster in pure aqueous solvent, so this estimate of τ^{298} should be considered to be approximate. Standard treatment of the data compiled in Fig. 5 yield rate coefficients of: $k_{ex}^{298} = 5 \times 10^3\ s^{-1}$ with $\Delta H^{\ddagger} = 33(\pm 2)$ kJ mol^{-1}, and $\Delta S^{\ddagger} = -64.6(\pm 7)$ J mol^{-1} K^{-1} in the mixed solvent. Observation of a contribution from the conjugate-base mechanism indicates that these activation parameters contain a small contribution from the enthalpy of deprotonation, which we do not attempt to constrain (see Casey and Sposito, 1992 for example).

The general timescale for proton exchange from the bound waters on the **Al$_{13}$** is on the order of a millisecond or less and compares well with timescales for fully protonated ions of trivalent metals. The *specific* proton lifetimes are most commonly reported and are easiest to compare. To make this comparison, it is conventional to normalize the lifetimes to the number of bound-water protons; for example, $\tau_{Al,H}^{298} = 12 \cdot \tau_{Al}^{298}$ for the $Al(OH_2)_6^{3+}$ ion because there are 12 protons that could exchange (two per bound water and six waters). The normalized lifetimes according to this procedure for the $Al(OH_2)_6^{3+}$, $Cr(OH_2)_6^{3+}$, and $Rh(OH_2)_6^{3+}$ ions are: 0.1×10^{-3}, 0.2×10^{-3}, and

7×10^{-3} s, respectively (see Swift and Stephenson, 1966; Stephenson et al., 1968; Fong and Grunwald, 1969; Bányai et al., 1995), and the value for bound waters on the **Al$_{13}$** is $\sim 5 \times 10^{-3}$ s.

The important point is that the bound waters on this large **Al$_{13}$** polyoxocation fall in the same general range as the simple monomers. It is likely that the lifetimes on structurally similar materials, such as the edges of aluminous clays and aluminum-hydroxide solids, will have similar proton lifetimes as well. The kinetics of these reactions seem to reflect short-range forces only. For example, Houston and Casey (2005) recently found that the lifetimes of a proton on waters bound to a trimeric oligomer were similar to those measured on the $Rh(H_2O)_6^{3+}$(aq) ion. It is, of course, difficult to scale the lifetimes for surfaces to the number of exchangeable protons, as is done when comparing oligomers to monomers, but the general lifetimes for an individual proton on a η-H_2O site bonded to a trivalent metal will fall into this familiar range of milliseconds and hundreds of microseconds.

4.2. Proton lifetimes on hydroxyl bridges (μ_2-OH)

The oxygen-exchange rates for sites in the **Al$_{13}$** are well known (Table 1) and comparison with the present results show that protons exchange many thousands of times from the hydroxyl bridges before an oxygen exchange event with bulk solvent. Oxygens in μ_2-OH^{slow} and μ_2-OH^{fast} sites within the **Al$_{13}$** exhibit lifetimes of $\tau^{298} \sim 17.4$ h and ~1 min, respectively, while the corresponding proton lifetimes at the two μ_2-OH sites are $\tau^{298} \sim 0.2$ and 0.013 s, respectively, in the mixed aqueous/organic solvents. The proton lifetimes are likely to be shorter in pure aqueous media, as indicated by the experiments in D_2O. These spectra contain a peak for only one μ_2-OH, which yielded an estimated τ^{298} of ~0.013 s. If this site corresponds to the more reactive of the two μ_2-OH, then the rates are unchanged in the various solvents. However, it is much more likely that this site is the less reactive μ_2-OH^{slow} site and that the peak for the second μ_2-OH^{fast} site is broadened beyond detection by rapid proton exchange. If so, then changing the solvent from a mixed water/organic solvent to D_2O causes rates to increase by a factor of 10–15.

The average lifetimes for hydroxyl protons in the **Al$_{13}$** are in the tens or hundreds of milliseconds at ambient temperatures, not microseconds or below, or seconds and greater. In the absence of any direct measurements, we expect similar average proton lifetimes for hydroxyl bridges on the aluminous basal plane of dioctahedral clays and aluminum-hydroxide solids. However, these lifetimes are shorter, by roughly an order of magnitude, than the relaxation times for desorption of a proton from a solid surface. These rates have been measured for ferric-, titanate-, and silicate-(hydr)oxide solids (see Astumian et al., 1981; Ikeda et al., 1982). The characteristic times for proton desorption at these uncharged surfaces fall into the range of: 0.1–10 s ($k_d^{int} = 0.16$–$46\ s^{-1}$; $0.004 \leqslant I \leqslant 0.002$; 298 K; see Table II in Astumian et al., 1981).

The proton lifetimes, we report here for the **Al$_{13}$** correspond to a dynamic equilibrium of proton exchanges between functional groups and bulk solution with no net change in charged state of the molecule. In contrast, the pressure-jump experiments of Astumian and coworkers (see Astumian et al., 1981; Ikeda et al., 1982) correspond to a net reaction (proton uptake or loss from the surface) that involves a net charging or discharging of the colloid surface (see Sparks, 1989 for details of the pressure-jump method). We speculate that the difference in timescales for the Brønsted reactions and the average proton lifetimes for the **Al$_{13}$** molecule are due to changes in hydration and electrolyte structures as charge moves near the oxide surface, although there are other complications as well (see Astumian and Schelley, 1984). It is surprising to us that the two timescales are so close.

The activation parameters for proton exchange at these bridges are clearly different than those for oxygen-isotope exchange (Table 1), as in the case of the bound waters. For exchange of oxygens, the activation enthalpies are $\Delta H^{\ddagger} = 202$ and 104 kJ mol^{-1}, respectively (Phillips et al., 2000; Casey et al., 2000). Using the data shown in Fig. 5, rate coefficients for proton exchange on the μ_2-OH^{fast} are: $k_{ex}^{298} = 79(\pm 30)\ s^{-1}$ with $\Delta H^{\ddagger} = 20.4(\pm 1)$ kJ mol^{-1}, and $\Delta S^{\ddagger} = -140(\pm 2)$ J mol^{-1} K^{-1}. Rate coefficients for proton exchange from the μ_2-OH^{slow} could only be estimated with two points and are: $k_{ex}^{298} = \sim 5\ s^{-1}$ with $\Delta H^{\ddagger} = 23$ kJ mol^{-1} and $\Delta S^{\ddagger} = -153$ J mol^{-1} K^{-1}. These activation enthalpies are much smaller than those for oxygen exchange (Table 1) and one includes a contribution of enthalpy from the Brønsted reactions, which we do not attempt to constrain here. They are, however, typical of proton-exchange reactions for ions, which fall in the range of $0 \leqslant \Delta H^{\ddagger} \leqslant 36$ kJ mol^{-1} and $10 \leqslant \Delta S^{\ddagger} \leqslant -180$ J mol^{-1} K^{-1} (e.g., Stephenson et al., 1968; Bányai et al., 1995).

5. Conclusions

The lifetimes of protons on the **Al$_{13}$** molecule have been estimated from ^{1}H NMR experiments which constrain the proton dynamics on the surfaces of aluminum-hydroxide materials. The average lifetime of a proton on η-H_2O at room temperature is in the submillisecond range and is not too different than that observed for other trivalent metal ions. The lifetimes for protons on the hydroxyl bridges, which are the first such measurements, are surprisingly long and fall into the range of tens to hundreds of milliseconds at room temperature. One μ_2-OH has a pH contribution to the proton-exchange reaction, but even if these data are extrapolated to a region with no pH dependence, the lifetimes are tens to a couple hundred milliseconds.

These lifetimes provide important constraints to dynamics at a mineral surface and suggest questions that could be explored by computation. For example, is there a structural reason for the difference in reactivity of the two μ_2-OH

sites? Does the less-labile site (μ_2-OH^{slow}) for oxygen-isotope exchange correspond to the μ_2-OH^{fast} for proton exchanges? Do rates correlate with an easily calculated property such as bond length? Do explicit interactions with the solvent need to be considered? The increase in rates for proton exchange at η-H_2O via the proton-enhanced pathway (k_2 in Eq. (4)) as pH is lowered are typically a factor of 2–3, not 200. Is the H_3O^+ ion directly involved in proton transfer or does it simply change the hydrogen-bonded structure of the solvation shell to better facilitate proton transfer to, and from, a H_2O? Finally, although steady-state proton transfer proceeds in fractions of a second, these rates are still slow on the computational time scale, as typical molecular-dynamic simulations extend only to nanoseconds. The exchange lifetimes illustrate the 'rare-event problem' for computational simulation of geochemical reactions. New algorithms need to be written to address these rare events in an accurate way that yields molecular rate information for reactions involving Earth materials.

Acknowledgments

The authors particularly thank three perceptive but anonymous referees who improved considerably the clarity of the text. Support for this research was from the US DOE via Grant DE-FG03-02ER15325 and from American Chemical Society (PRF Grant: 40412-AC2). The NMR spectrometer was purchased using Grant OSTI 97-24412. The authors benefited from discussion with Prof. James Rustad on proton transfer and simulation and, as always, with Prof. Gerhard Furrer on the general chemistry of this molecule.

Associate editor: Garrison Sposito

References

Akitt, J.W., 1989. Multinuclear studies of aluminum compounds. *Prog. NMR Spectrosc.* **21**, 1–149.

Akitt, J.W., Elders, J.M., 1988. Multinuclear magnetic resonance studies of the hydrolysis of aluminum(III). Part 8. Base hydrolysis monitored at very high magnetic field. *J. Chem. Soc. Dalton Trans.* **1988**, 1347–1355.

Amirbahman, G., Gfeller, M., Furrer, G., 2000. Kinetics and mechanism of ligand-promoted decomposition of the Keggin Al-13 polymer. *Geochim. Cosmochim. Acta* **64**, 911–919.

Astumian, R.D., Sasaki, M., Yasunaga, T., Schelly, Z.A., 1981. Proton adsorption–desorption kinetics at iron oxides in aqueous suspensions, using the pressure-jump method. *J. Phys. Chem.* **85**, 3832–3835.

Astumian, R.D., Schelley, Z.A., 1984. Geometric effects of reduction of dimensionality in interfacial reactions. *J. Am. Chem. Soc.* **106**, 304–308.

Bányai, I., Glaser, J., Read, J.C., Sandström, M., 1995. Slow proton exchange kinetics in aqueous solutions of hexaaquarhodium(III): influence of the second hydration shell. *Inorg. Chem.* **34**, 2423–2429.

Bleuzen, A., Pittet, P.-A., Helm, L., Merbach, A.E., 1997. Water exchange on magnesium(II) in aqueous solution: a variable temperature and pressure ^{17}O NMR study. *Magn. Reson. Chem.* **35**, 765–773.

Bradley, S.M., Kydd, R.A., Howe, R.F., 1993. The structure of aluminum gels formed through the base hydrolysis of Al^{3+} aqueous solutions. *J. Colloid Interface Sci.* **159**, 405–412.

Casey, W.H., Phillips, B.L., 2001. Kinetics of oxygen exchange between sites in the $GaO_4Al_{12}(OH)_{24}(H_2O)_{12}^{7+}$(aq) molecule and aqueous solution. *Geochim. Cosmochim. Acta* **65**, 705–714.

Casey, W.H., Sposito, G., 1992. On the temperature dependence of mineral dissolution rates. *Geochim. Cosmochim. Acta* **56**, 3825–3830.

Casey, W.H., Phillips, B.L., Karlsson, M., Nordin, S., Nordin, J.P., Sullivan, D.J., Neugebauer-Crawford, S., 2000. Rates and mechanisms of oxygen exchanges between sites in the $AlO_4Al_{12}(OH)_{24}(H_2O)_{12}^{7+}$(aq) complex and water: implications for mineral surface chemistry. *Geochim. Cosmochim. Acta* **64**, 2951–2964.

Casey, W.H., Swaddle, T.W., 2003. Why small? The use of small inorganic clusters to understand mineral surface and dissolution reactions in geochemistry. *Rev. Geophys.* **41**, 1–20.

Fong, D.-W., Grunwald, E., 1969. Kinetic study of proton exchange between the $Al(OH_2)_6^{3+}$ ion and water in dilute acid. Participation of water molecules in proton transfer. *J. Am. Chem. Soc.* **91**, 2413–2422.

Furrer, G., Ludwig, Chr., Schindler, P.W., 1992. On the chemistry of the Keggin Al-13 polymer. *J. Colloid Interface Sci.* **149**, 56–67.

Furrer, G., Gfeller, M., Wehrli, B., 1999. On the chemistry of the Keggin Al-13 polymer: kinetics of proton-promoted decomposition. *Geochim. Cosmochim. Acta* **63**, 3069–3076.

Furrer, G., Phillips, B.L., Ulrich, K.-U., Pöthig, R., Casey, W.H., 2002. The origin of aluminum flocs in polluted streams. *Science* **297**, 2245–2247.

Hiemstra, T., Yong, H., Van Riemsdijk, W.H., 1999. Interfacial charging behavior of aluminum (hydr)oxides. *Langmuir* **15**, 5942–5955.

Houston, J.R., Casey, W.H., 2005. Proton exchange kinetics from the bound waters on the oxo-centered rhodium(III) trimer $[Rh_3(\mu_3\text{-}O)(\mu\text{-}O_2CCH_3)_6(OH_2)_3]^+$: a variable pH and temperature ^1H NMR study. *Dalton Trans.* **2005**, 3667–3671.

Ikeda, T., Sasaki, M., Hachiya, K., Astumian, R.D., Yasunaga, T., Schelly, Z.A., 1982. Adsorption–desorption kinetics of acetic acid on silica–alumina particles in aqueous suspensions, using the pressure-jump relaxation method. *J. Phys. Chem.* **86**, 3861–3866.

Lee, A.P., Phillips, B.L., Casey, W.H., 2002a. The kinetics of oxygen exchange between the $GeO_4Al_{12}(OH)_{24}(OH_2)_{12}^{8+}$(aq) molecule and aqueous solutions. *Geochim. Cosmochim. Acta* **66**, 577–587.

Lee, A.P., Furrer, G., Casey, W.H., 2002b. On the acid–base chemistry of the Keggin polymers: $GaAl_{12}$ and $GeAl_{12}$. *J. Colloid Interface Sci.* **250**, 269–270.

Phillips, B.L., Casey, W.H., Karlsson, M., 2000. Bonding and reactivity at oxide mineral surfaces from model aqueous complexes. *Nature* **404**, 379–382.

Rustad, J.R., Loring, J.L., Casey, W.H., 2004. Oxygen-exchange pathways in aluminum polyoxocations. *Geochim. Cosmochim. Acta* **68**, 3011–3017.

Sandström, J., 1982. *Dynamic Nuclear Magnetic Resonance Spectroscopy*. Academic Press, London, 221 pp.

Sparks, D.L., 1989. *Kinetics of Soil Chemical Processes*. Academic Press, New York, p. 210.

Stephenson, T.A., Swift, T.J., Spencer, J.B., 1968. Aquated cations in aqueous solution and the kinetics of proton transfer. *J. Am. Chem. Soc.* **90**, 4291–4296.

Swaddle, T.S., Rosenqvist, J.R., Yu, P., Bylaska, E., Phillips, B.L., Casey, W.H., 2005. Kinetic evidence for five-coordinated $AlOH^{2+}$ ion. *Science* **308**, 1450–1452.

Swift, T.J., Stephenson, T.A., 1966. The kinetics of protonation of nickel and chromium hexaaquo cations in aqueous solution. *Inorg. Chem.* **5**, 1100–1105.